Polymer 50 (2009) 1692–1699

Contents lists available at ScienceDirect

Polymer

journal homepage: www.elsevier.com/locate/polymer

Electrochemically and electrochromically stable polyimides bearing *tert*-butyl-blocked *N*,*N*,*N*′,*N*′-tetraphenyl-1,4-phenylenediamine units

Hui-Min Wang, Sheng-Huei Hsiao*

Department of Chemical Engineering and Biotechnology, National Taipei University of Technology, 1 Chunghsiao East Road, Section 3, Taipei 10608, Taiwan, ROC

ARTICLE INFO

Article history:
Received 2 January 2009
Accepted 10 February 2009
Available online 14 February 2009

Keywords:
Polyimides
Triphenylamine
Electroactivity

ABSTRACT

A new class of electrochemically active polyimides with di-*tert*-butyl-substituted *N*,*N*,*N*′,*N*′-tetraphenyl-1,4-phenylenediamine units was prepared from *N*,*N*-bis(4-aminophenyl)-*N*′,*N*′-bis(4-*tert*-butylphenyl)-1,4-phenylenediamine and various aromatic tetracarboxylic dianhydrides *via* a conventional two-step procedure that included a ring-opening polyaddition to give poly(amic acid)s, followed by chemical or thermal cyclodehydration. Most of the polyimides are readily soluble in many organic solvents and can be solution-cast into tough and amorphous films. They had useful levels of thermal stability, with relatively high glass-transition temperatures (276–334 °C), 10% weight-loss temperatures in excess of 500 °C, and char yields at 800 °C in nitrogen higher than 60%. Cyclic voltammograms of the polyimide films cast on the indium-tin oxide (ITO)-coated glass substrate exhibited two reversible oxidation redox couples at 0.70–0.74 V and 1.05–1.08 V vs. Ag/AgCl in acetonitrile solution. The polyimide films revealed excellent stability of electrochromic characteristics, with a color change from colorless or pale yellowish neutral form to green and blue oxidized forms at applied potentials ranging from 0.0 to 1.3 V. These anodically coloring polymeric materials exhibited high optical contrast of percentage transmittance change ($\Delta\%T$) up to 44% at 413 nm and 43% at 890 nm for the green coloration, and 98% at 681 nm for the blue coloration. After over 50 cyclic switches, the polymer films still exhibited good redox and electrochromic stability.

1. Introduction

Electrochromism is known as the evocation or alternation of color by passing a current or applying a potential [1,2]. This interesting property led to the development of many technological applications such as self-darkening rear-view mirrors, adjustably darkening windows, large-scale electrochromic screens, and chameleon materials [3–7]. There are many chemical systems that are intrinsically electrochromic, such as metal oxides, metal-organic complexes, and conjugated conductive polymers [7,8]. Conjugated electroactive polymers offer a broad set of new materials for electrochromic applications. These polymers exhibit ease of processability and useful mechanical properties (e.g. flexibility). However, the major advantage of these organic-based materials is that their electrochromic properties (switching speed, contrast ratio, and color) can be tuned through chemical structure modification [9–12]. The Reynolds group has carried out extensive studies on the design and synthesis of poly(3,4-alkylenedioxythiophene)s and poly(3,4-alkylenedioxypyrrole)s based polymers for electrochromic applications [13–15].

It is well known that aromatic polyimides offer a combination of outstanding properties such as chemical and thermal stabilities, electric and mechanical properties, gas separation characteristics, etc.; therefore, they have been widely used in microelectronics, optoelectronics, and aerospace engineering [16–18]. However, they are difficult to process in their fully imidized form because of high softening temperatures and limited solubility in commercially available solvents, thus possibly narrowing down their applicability. Therefore, various efforts have focused on the design and preparation of processable polyimides while maintaining their excellent properties [19,20]. One of the common approaches for increasing solubility and processability of polyimides without sacrificing high thermal stability is the introduction of bulky, packing-disruptive groups into the polymer backbone [21–29]. Incorporating the three-dimensional, propeller-shaped triphenylamine (TPA) unit into polymer backbone has been demonstrated to be a unique approach to enhance the solubility of polyimides [30–33]. Furthermore, TPA-based polymers have been widely used as the hole-transport materials in EL devices, and they also have been found to show interesting electrochromic behavior [34–36].

* Corresponding author. Tel.: +886 2 27712171; fax: +886 2 27317117.
E-mail address: shhsiao@ntut.edu.tw (S.-H. Hsiao).

0032-3861/$ – see front matter © 2009 Elsevier Ltd. All rights reserved.
doi:10.1016/j.polymer.2009.02.009

The anodic oxidation pathways of TPA have been well investigated [37]. Unsubstituted TPA undergoes coupling deprotonation to form tetraphenylbenzidine after the formation of the initial monocation radical. It has been well established that incorporation of electron-donating substituents at the *para*-position of TPA affords stable radical cations [38–40]. The redox properties, ion-transfer process, and electrochromic behavior of *N*,*N*,*N*′,*N*′-tetraphenyl-1,4-phenylenediamine (TPPA) derivatives are important for technological application [41]. Recently, the Liou group has reported that aromatic polyamides containing TPPA moieties reveal interesting electrochromic characteristics, such as polyelectrochromism, high coloration efficiency, fast switching time, high optical contrast, and excellent redox stability [42–44]. As part of our continued interest in electroactive high-performance polymers, we report the synthesis and characterization of a new family of TPPA-containing aromatic polyimides based on *N*,*N*-bis(4-aminophenyl)-*N*′,*N*′-bis(4-*tert*-butylphenyl)-1,4-phenylenediamine (**4**). With such a configuration, the electrochemically active sites of the pendent phenyl groups of the TPPA unit are blocked, giving the polyimides extra electrochemical stability. Therefore, these polyimides are expected to possess an enhanced redox and electrochromic stability.

2. Experimental

2.1. Materials

N,*N*-Bis(4-aminophenyl)-*N*′,*N*′-bis(4-*tert*-butylphenyl)-1,4-phenylenediamine (**4**) was synthesized by a well-known synthetic route starting from bis(4-*tert*-butylphenyl)amine and *p*-fluoronitrobenzene as shown in Scheme 1. The synthetic details and the characterization data of this diamine monomer have been described in a separate paper [45]. *N*,*N*-Dimethylacetamide (DMAc) was dried over calcium hydride for 24 h, distilled under reduced pressure, and stored over 4 Å molecular sieves in a sealed bottle. Commercially available tetracarboxylic dianhydrides such as pyromellitic dianhydride (PMDA; **5a**; Aldrich) and 3,3′,4,4′-benzophenonetetracarboxylic dianhydride (BTDA; **5c**; Aldrich) were purified by recrystallization from acetic anhydride. The other dianhydrides that included 3,4,3′,4′-biphenyltetracarboxylic dianhydride (BPDA; **5b**; Oxychem), 4,4′-oxydiphthalic dianhydride (ODPA; **5d**; Oxychem), 3,4,3′,4′-diphenylsulfonetetracarboxylic dianhydride (DSDA; **5e**; New Japan Chemical Co.), and 2,2-bis(3,4-dicarboxyphenyl)hexafluoropropane dianhydride (6FDA; **5f**; Hoechst Celanese) were heated at 250 °C *in vacuo* for 3 h before use. Tetra-*n*-butylammonium perchlorate (TBAP) was obtained from Acros and recrystallized twice from ethyl acetate and then dried under vacuum before use. All other reagents were used as received from commercial sources.

2.2. Polymer synthesis

The polyimides **6a**–**6f** were synthesized from diamine **4** and dianhydrides **5a**–**5f** by the conventional two-step method *via* thermal and chemical imidization reaction. A typical procedure is as follows. The diamine monomer **4** (0.8330 g, 1.501 mmol) was dissolved in 14.2 mL of DMAc in a 50-mL round-bottom flask. Then dianhydride 6FDA (**5f**) (0.6670 g, 1.501 mmol) was added to the diamine solution in one portion. Thus, the solid content of the reaction solution is approximately 10 wt%. The mixture was stirred at room temperature for about 12 h to yield a viscous poly(amic acid) solution. The inherent viscosity of the resulting poly(amic acid) was 0.67 dL/g, measured in DMAc at a concentration of 0.5 g/dL at 30 °C. For the thermal imidization process, about 7 g of the obtained poly(amic acid) solution was transferred to a 9-cm glass Petri dish, which was placed overnight in a 90 °C oven for the slow release of the casting solvent. The poly(amic acid) in the form of solid film was converted to polyimide **6f** by successive heating under vacuum at 150 °C for 30 min, 200 °C for 30 min, and then 250 °C for 1 h. For X-ray diffraction and thermal analyses, the polyimide films were further heated at 300 °C for 1 h. For the chemical imidization method, 4 mL of acetic anhydride and 2 mL of pyridine were added to the remaining poly(amic acid) solution, and the mixture was heated at 100 °C for 1 h to effect a complete imidization. The homogenous polymer solution was poured slowly into 200 mL of stirring methanol giving rise to a beige precipitate that was collected by filtration, washed thoroughly with hot water and methanol, and dried. A polymer solution was made by the dissolution of about 0.5 g of the polyimide sample in 10 mL of hot DMAc. The homogeneous solution was poured into a 9-cm glass Petri dish, which was placed in a 90 °C oven overnight for the slow release of the solvent, and then the film was stripped off from the glass substrate and further dried in vacuum at 160 °C for 6 h. The IR spectrum of **6f** (film) exhibited characteristic imide absorption

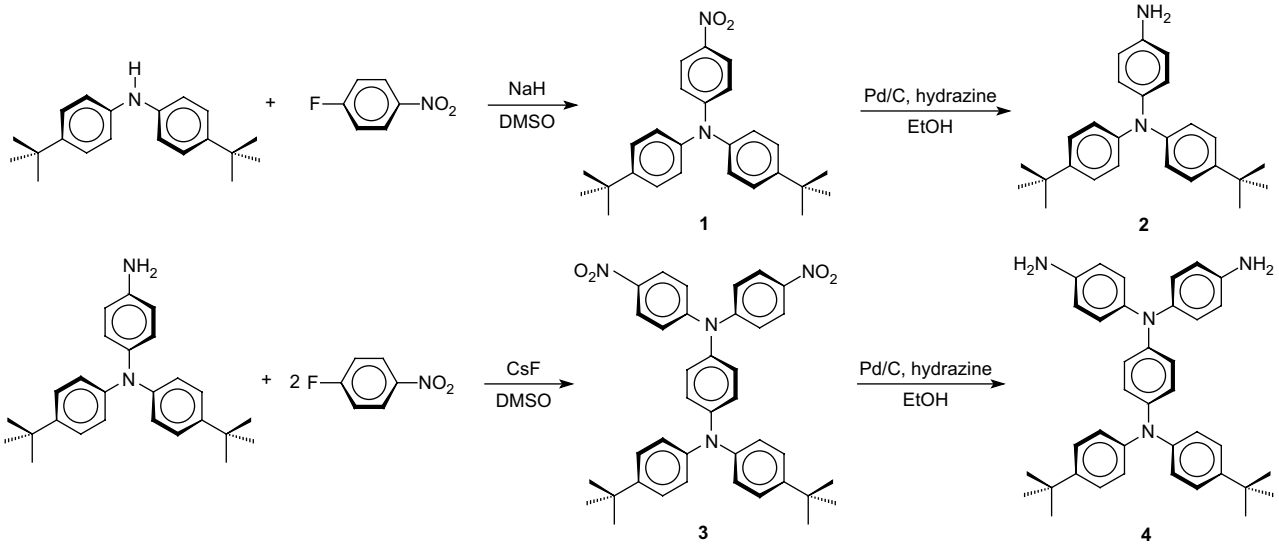

Scheme 1. Synthetic route to the diamine monomer **4**.

bands at 1780 (asymmetrical C=O stretch) and 1732 cm^{-1} (symmetrical C=O stretch).

2.3. Measurements

Infrared (IR) spectra were recorded on a Horiba FT-720 FT-IR spectrometer. Elemental analyses were run in a Heraeus VarioEL III CHNS elemental analyzer. ^1H and ^{13}C NMR spectra were measured on a Bruker AVANCE 500 FT-NMR system with tetramethylsilane as an internal standard. The inherent viscosities were determined with an Ubbelohde viscometer at 30 °C. Weight-average molecular weights (M_w) and number-average molecular weights (M_n) were obtained *via* gel permeation chromatography (GPC) on the basis of polystyrene calibration using Waters 2410 as an apparatus and THF as the eluent. Wide-angle X-ray diffraction (WAXD) measurements were performed at room temperature (ca. 25 °C) on a Shimadzu XRD-6000 X-ray diffractometer with a graphite monochromator (operating at 40 kV and 30 mA), using nickel-filtered Cu-Kα radiation ($\lambda = 1.5418$ Å). The scanning rate was 2°/min over a range of $2\theta = 10$–40°. Ultraviolet–visible (UV–vis) spectra of the polymer films were recorded on a Jasco UV/VIS V530 spectrometer. Thermogravimetric analysis (TGA) was performed with a Perkin–Elmer Pyris 1 TGA. Experiments were carried out on approximately 4–6 mg of samples heated in flowing nitrogen or air (flow rate = 40 cm^3/min) at a heating rate of 20 °C/min. DSC analyses were performed on a Perkin–Elmer Pyris 1 DSC at a scan rate of 20 °C/min in flowing nitrogen. Thermomechanical analysis (TMA) was determined with a Perkin–Elmer TMA 7 instrument. The TMA experiments were carried out from 50 to 400 °C at a scan rate of 10 °C/min with a penetration probe 1.0 mm in diameter under an applied constant load of 10 mN. Softening temperatures (T_s) were taken as the onset temperatures of probe displacement on the TMA traces. Electrochemistry was performed with a CHI 611C electrochemical analyzer. Voltammograms are presented with the positive potential pointing to the left and with increasing anodic currents pointing downwards. Cyclic voltammetry (CV) was conducted with the use of a three-electrode cell in which ITO (polymer films area about 0.8 cm × 1.25 cm) was used as a working electrode. A platinum wire was used as an auxiliary electrode. All cell potentials were taken with the use of a home-made Ag/AgCl, KCl (sat.)

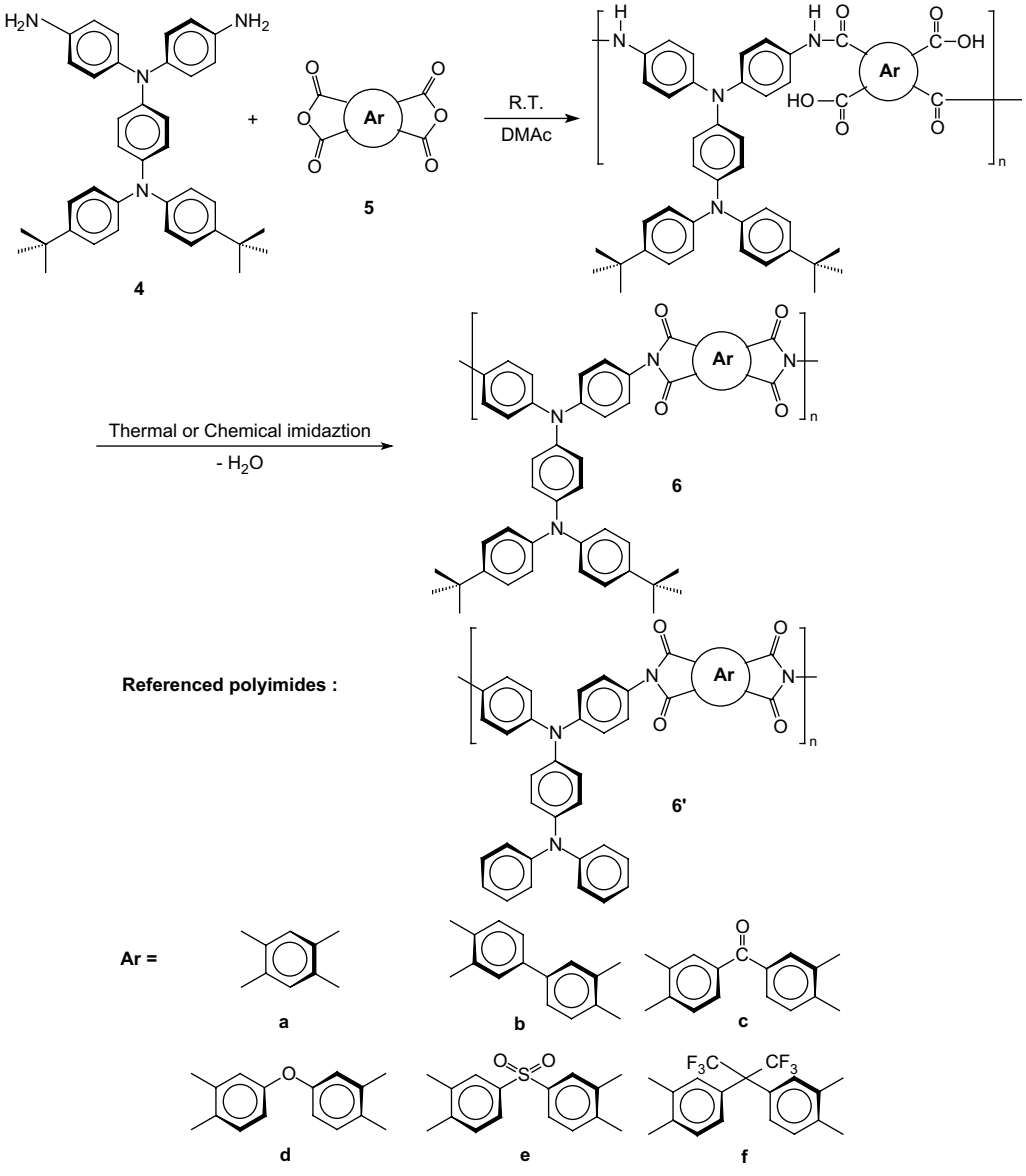

Scheme 2. Synthesis of polyimides **6a**–**6f**.

Table 1
Inherent viscosity and solubility behavior of polyimides prepared *via* thermal (-T) or chemical (-C) imidization.

Polymer code	η_{inh}[a] (dL/g)		Solvents[b]					
	PAA	Polyimide	NMP	DMAc	DMF	DMSO	*m*-Cresol	THF
6a-T	1.11	–	±	±	±	–	+	±
6a-C		–	±	±	±	–	±	±
6b-T	0.92	–	±	±	±	–	+	±
6b-C		–	±	±	±	–	±	±
6c-T	0.65	–	+	±	±	–	+	+
6c-C		–	++	±	±	–	++	+
6d-T	0.81	0.44	++	++	±	–	++	+
6d-C		0.40	++	++	±	–	++	++
6e-T	0.56	0.32	++	++	++	±	++	++
6e-C		0.40	++	++	++	±	++	++
6f-T	0.67	0.33	++	++	++	±	++	++
6f-C		0.57	++	++	++	±	++	++

[a] Inherent viscosity measured at a concentration of 0.5 dL/g in DMAc at 30 °C. PAA: poly(amic acid).
[b] The qualitative solubility was tested with 10 mg of a sample in 1 mL of stirred solvent. ++, Soluble at room temperature; +, soluble on heating; ±, partially soluble; –, insoluble even on heating. NMP: *N*-methyl-2-pyrrolidone; DMAc: *N*,*N*-dimethylacetamide; DMF: *N*,*N*-dimethylformamide; DMSO: dimethyl sulfoxide; THF: tetrahydrofuran.

reference electrode. Ferrocene was used as an external reference for calibration (+0.48 V vs. Ag/AgCl). Spectroelectrochemistry analyses were carried out with an electrolytic cell, which was composed of a 1-cm cuvette, ITO as a working electrode, a platinum wire as an auxiliary electrode, and an Ag/AgCl reference electrode. Absorption spectra in the spectroelectrochemical experiments were measured with an Agilent 8453 UV–Visible spectrophotometer. Coloration efficiency is calculated from the equation: $\eta = \Delta OD/Q$, where ΔOD is optical density change at specific absorption wavelength and Q is ejected charge determined from the *in situ* experiments [46,47]. Photoluminescence (PL) spectra were measured with a Varian Cary Eclipse fluorescence spectrophotometer. Fluorescence quantum yields (Φ_F) values of the samples in NMP were measured by using quinine sulfate in 1 N H_2SO_4 as a reference standard ($\Phi_F = 54.6\%$) [48].

3. Results and discussion

3.1. Polymer synthesis

Polyimides **6a**–**6f** were prepared in conventional two-step method by the reactions of equal molar amounts of diamine monomer **4** with various aromatic dianhydrides (**5a**–**5f**) to form poly(amic acid)s, followed by thermal or chemical cyclodehydration (Scheme 2). As shown in Table 1, the inherent viscosities of the precursor poly(amic acid)s ranged from 0.56 to 1.11 dL/g. The molecular weights of all the poly(amic acid)s were sufficiently high to permit the casting of flexible and strong poly(amic acid) films. The thermal conversion to polyimides was carried out by successive heating of the poly(amic acid) films to 250 °C *in vacuo*. The poly(amic acid) precursors also could be chemically dehydrated to the polyimides by treatment with acetic anhydride and pyridine. All polyimides except **6a** could afford flexible and tough films. The film of **6a** might crack on fingernail creasing because of structural rigidity of its polymer backbone. Table 2 shows the molecular weights of the chemically imidized samples of **6e** and **6f** measured by GPC using polystyrenes as standard and THF as solvent. These two polyimides exhibited weight-average molecular weights (M_w) of 66,500 and 88,500 with polydispersity index (M_w/M_n) of 1.48 and 1.38, respectively. The formation of polyimides was confirmed with IR spectroscopy. All the polyimides showed the characteristic absorption bands of the imide ring near 1780 (asymmetric C=O stretching) and 1730 cm^{-1} (symmetric C=O stretching). Typical IR spectra of polyimide **6a** and its poly(amic acid) precursor are illustrated in Fig. 1. The disappearance of amide and carboxyl bands indicated a virtually complete conversion of the poly(amic acid) precursor to the polyimide.

Table 2
GPC data of polyimides **6e** and **6f** prepared *via* chemical imidization.

Polymer	M_w[a]	M_n[a]	PDI[b]	DP[c]
6e-C	66,500	45,000	1.48	76
6f-C	88,500	64,000	1.38	92

[a] Average molecular weights relative to polystyrene standard by GPC, using THF as the eluent.
[b] Polydispersity index = M_w/M_n.
[c] Estimated degree of polymerization.

3.2. Polymer properties

3.2.1. Solubility and film morphology

The solubility behavior of polymers **6a**–**6f** obtained by thermal or chemical imidization was investigated qualitatively, and the results are also listed in Table 1. The solubility behavior of the polyimides depended on their chain packing ability and intermolecular interactions that was affected by the rigidity, symmetry, and

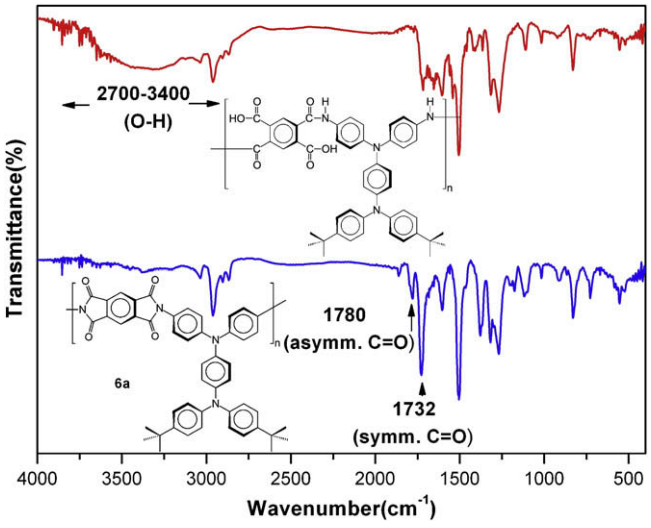

Fig. 1. Typical IR spectra of the polyimide **6a** and its poly(amic acid) precursor.

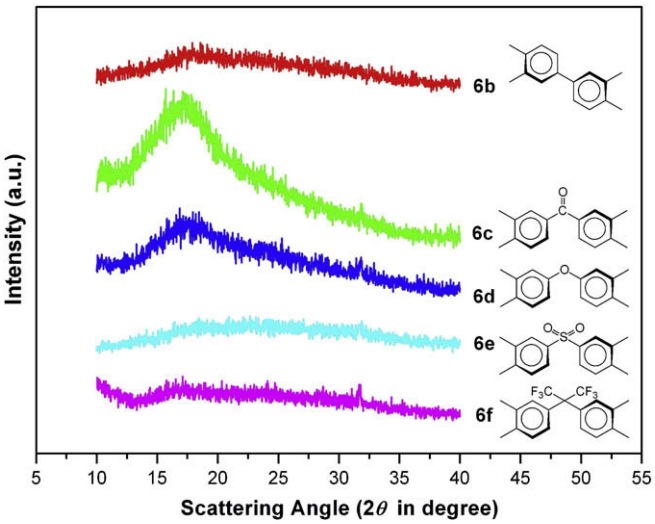

Fig. 2. WAXD patterns of the thin films of polyimides **6b**–**6f**.

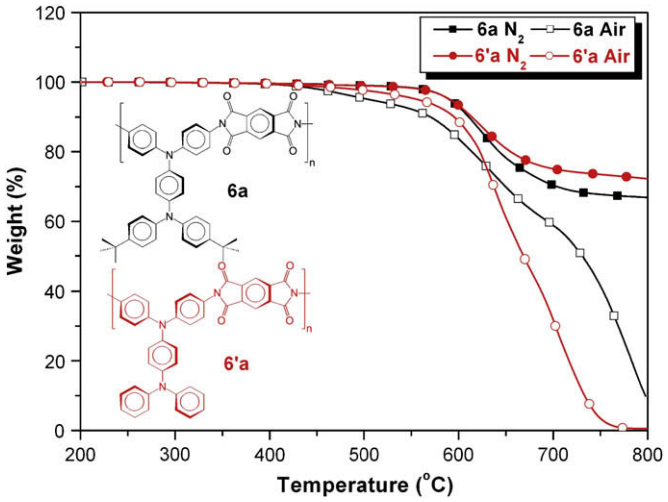

Fig. 3. TGA curves of polyimides **6a** and **6′a** with a heating rate of 20 °C/min.

regularity of the molecular backbone. The polyimides (**6a**–**6c**) derived from more rigid dianhydrides, such as PMDA, BPDA, and BTDA, showed a relatively lower solubility than the others. In contrast, polyimides **6d**–**6f** revealed good solubility in common organic solvents such as NMP, DMAc, DMF, *m*-cresol, and THF at room temperature and could be solution-cast to tough and transparent films in the fully imidized form. In addition, the polyimides prepared by the chemical imidization method exhibited a slightly higher solubility as compared with those by the two-step thermal imidization method. For example, polyimide **6c-C** could be readily soluble in NMP and *m*-cresol at room temperature, whereas **6c-T** was only soluble upon heating in these two solvents. Thus, the difference in solubility of these polyimides obtained by different methods could be ascribed to morphological change of the polymers during heat treatment resulting in some degree of ordering from molecular aggregation of the polymer chain segments. As shown in Fig. 2, all the polyimides showed amorphous wide-angle X-ray diffraction (WAXD) patterns. Their amorphous properties can be attributed to the incorporation of bulky *tert*-butyl substitutents and packing-disruptive TPPA unit along the polymer backbone, which results in a high steric hindrance for close packing and thus reduces their crystallization tendency.

3.2.2. Thermal properties

The thermal behavior data of polyimides **6a**–**6f** together with their referenced analogs **6′a**–**6′f** are included in Table 3. Typical TGA curves of representative polyimides **6a** and **6′a** in both air and nitrogen atmospheres are shown in Fig. 3. All of the polyimides exhibited a similar TGA pattern with no significant weight loss below 500 °C in air or nitrogen atmosphere. The decomposition temperatures (T_d) at which a 10% weight-loss temperatures of the **6** series polyimides in nitrogen and air were recorded in the range of 538–632 °C and 519–585 °C, respectively. The amount of carbonized residue (char yield) of these polymers in nitrogen atmosphere was more than 60% at 800 °C. The high char yields of these polymers can be ascribed to their high aromatic content. All the **6** series polyimides exhibited a lower T_d value as compared with their corresponding counterparts without the *tert*-butyl group. This is reasonable when considering the less stable aliphatic segments.

The glass-transition temperatures (T_gs) of all the polymers were observed in the range of 276–334 °C by DSC. The decreasing order of T_g generally correlated with that of chain flexibility. For example, the polyimide **6d** from ODPA showed the lowest T_g (276 °C) because of the presence of flexible ether linkage between the phthalimide units. All the polymers indicated no clear melting endotherms up to the decomposition temperatures on the DSC thermograms. This result also supports the amorphous nature associated with these polymers. The softening temperatures (T_s) (may be referred to as apparent T_g) of the polymer film samples were determined by the TMA method with a loaded penetration probe. They were obtained from the onset temperature of the probe displacement on the TMA trace. A typical TMA thermogram for polyimide **6d** is illustrated in Fig. 4, where the DSC curve of this polymer is also included as an

Table 3
Thermal properties of polyimides[a].

Polymer code	T_g[b] (°C)	T_s[c] (°C)	T_d[d] at 10 wt% loss (°C)		Char yield[e] (wt%)
			In N_2	In air	
6a	334 (352)[f]	300 (327)	611 (614)	570 (595)	67 (72)
6b	311 (302)	291 (267)	632 (629)	584 (622)	75 (70)
6c	295 (294)	281 (251)	607 (618)	563 (589)	75 (63)
6d	276 (264)	262 (258)	613 (610)	585 (600)	67 (74)
6e	305 (305)	279 (281)	538 (568)	519 (582)	60 (67)
6f	294 (286)	273 (261)	608 (585)	578 (574)	65 (68)

[a] The polymer film samples were heated at 300 °C for 1 h prior to all the thermal analyses.
[b] Midpoint temperature of the baseline shift on the second DSC heating trace (rate = 20 °C/min) of the sample after quenching from 400 to 50 °C (rate = −200 °C/min) in nitrogen.
[c] Softening temperature measured by TMA with a constant applied load of 10 mN at a heating rate of 10 °C/min.
[d] Decomposition temperature, recorded *via* TGA at a heating rate of 20 °C/min and a gas-flow rate of 30 cm^3/min.
[e] Residual weight percentage at 800 °C in nitrogen.
[f] Data in parentheses are those of structurally similar polyimides **6′a**–**6′f** without the *tert*-butyl substituent.

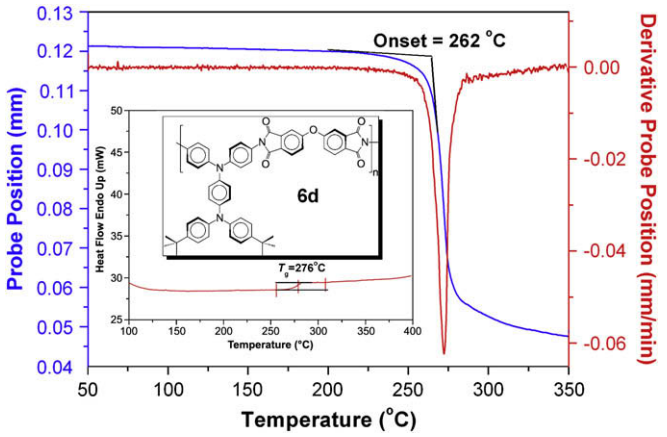

Fig. 4. TMA and DSC curves of polyimide **6d** with a heating rate of 10 and 20 °C/min, respectively.

inset. The T_s values obtained by TMA were recorded in the 262–300 °C range. Except for **6a**, the other **6** series polyimides revealed a similar or slightly higher T_g and T_s value when compared to their respective **6′** analogs. The increased T_g implies that the bulky *tert*-butyl substituent in the former leads to an increase in steric hindrance for chain mobility.

3.2.3. Optical and electrochemical properties

The optical properties of the polyimides were investigated by UV–vis and photoluminescence (PL) spectroscopy. The results are summarized in Table 4. The polymers exhibited UV–vis absorption bands with λ_{max} at 302–323 nm in NMP solutions, assignable mainly to the combinations of n–π^* and π–π^* transitions resulting from the conjugated TPPA segment. In the solid film, the polyimides showed absorption characteristics (λ_{max} around 310–344 nm) similar to those in the solution. Fig. 5 shows solution UV–vis absorption and PL emission spectra of polyimides **6e** and **6f** in NMP at a concentration of around 1×10^{-5} mol/L. These polyimides exhibited a violet–blue fluorescence emission maximum at around 366–414 nm in dilute NMP solution. The low fluorescence quantum yield of these polyimides may be attributed to the quenching effect arising from intermolecular charge transfer complexing between the TPPA donor and the imide acceptor.

The electrochemical behavior of the polyimides was investigated by CV conducted for a cast film on the ITO-coated glass substrate as working electrode in dry acetonitrile (CH_3CN) containing 0.1 M of TBAP as the supporting electrolyte and saturated

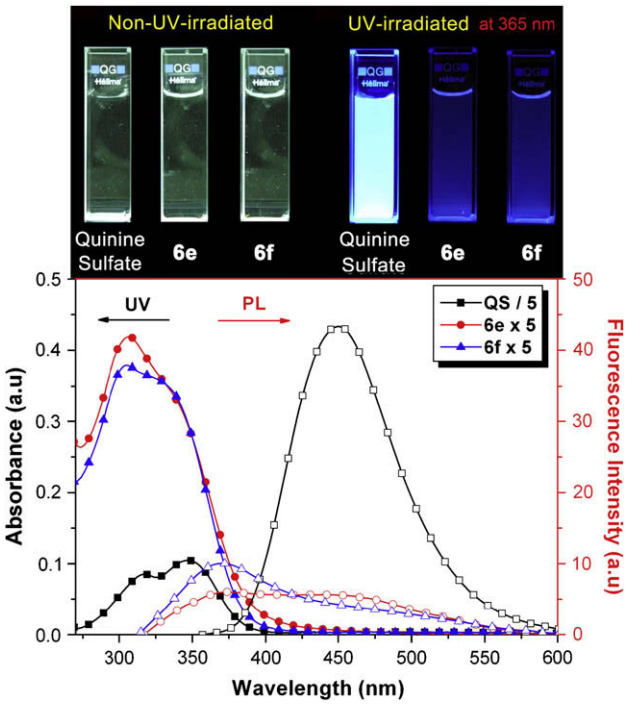

Fig. 5. UV–vis and PL spectra of solutions of polyimides **6e** and **6f** in NMP (1×10^{-5} M). A solution of quinine sulfate in 1 N H_2SO_4 (aq) with a concentration of 1×10^{-5} M was used as the reference standard ($\Phi_F = 0.546$). Photographs show the appearance of the sample solutions before and after exposure to a standard laboratory UV lamp.

Ag/AgCl as the reference electrode under nitrogen atmosphere. All the **6** series polyimides exhibited two reversible oxidative processes as evidenced by their CV curves. The typical cyclic voltammograms for the representative polyimide **6e** are illustrated in Fig. 6. There are two reversible oxidation redox couples at half-wave potentials ($E_{1/2}$) of 0.73 V ($E_{onset} = 0.60$ V) and 1.06 V for polyimide **6e** in the oxidative scan. The color of the film changed from colorless to green and then blue as a result of electrochemical oxidation of the TPPA moiety. Because of the stability of the films and the good adhesion between the polymer and ITO substrate, the polyimide **6e** exhibited excellent reversibility of electrochromic characteristics during fifty repeated cyclic scans between 0.0 and 1.3 V, changing color from colorless to green then blue at electrode potentials ranging from 0.73 V to 1.06 V. The first electron removal for polyimide **6e** is assumed to occur at the nitrogen atom on the pendent 4,4′-di-*tert*-butyltriphenylamine group, which is more

Table 4
Optical and electrochemical properties of the polyimides.

Polymer code	In solution			As film		Oxidation potential[c] (V) (vs. Ag/AgCl in CH_3CN)			E_g[d] (eV)	HOMO[e] (eV)		LUMO[e] (eV)	
	abs λ_{max} (nm)[a]	PL λ_{max} (nm)[a]	Φ_F[b] (%)	abs λ_{max} (nm)	abs λ_{onset} (nm)	First		Second		E_{onset}	$E_{1/2}$	E_{onset}	$E_{1/2}$
						E_{onset}	$E_{1/2}$	$E_{1/2}$					
6a	302	366	1.17	344	437	0.57	0.73	1.07	2.84	4.93	5.09	2.09	2.25
6b	323	405	0.32	330	415	0.57	0.74	1.08	2.99	4.93	5.10	1.94	2.11
6c	312	378	0.50	326	423	0.64	0.74	1.07	2.93	5.00	5.10	2.07	2.17
6d	319	378	0.63	338	416	0.65	0.74	1.05	2.98	5.01	5.10	2.03	2.12
6e	307	374	0.52	310	428	0.60	0.73	1.06	2.90	4.96	5.09	2.06	2.19
6f	305	370	0.64	342	423	0.65	0.74	1.06	2.93	5.01	5.10	2.08	2.17
6′e	309	426	0.30	317	418	0.63	0.74	1.10	2.97	4.99	5.10	2.02	2.13

[a] Measured in dilute solution in NMP at a concentration of about 10^{-5} mol/L.
[b] The quantum yield in dilute solution was calculated in an integrating sphere with quinine sulfate as the standard ($\Phi_F = 54.6\%$).
[c] Oxidation potentials from cyclic voltammograms.
[d] Energy gap = 1240/abs λ_{onset} of the polymer film.
[e] The HOMO energy levels were calculated from E_{onset} or $E_{1/2}$ and were referenced to ferrocene (4.8 eV). LUMO = HOMO − E_g.

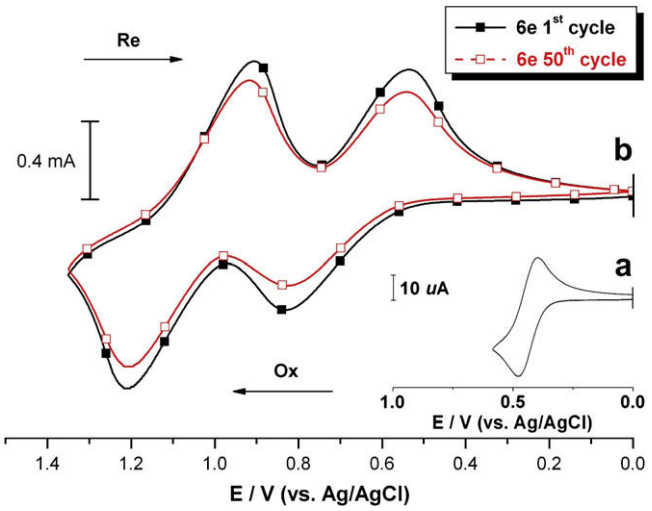

Fig. 6. Cyclic voltammograms of (a) ferrocene and (b) the cast film of polyimide **6e** on the ITO-coated glass slide in CH_3CN containing 0.1 M TBAP at scan rate of 0.1 V/s.

electron-rich than the nitrogen atom on the main-chain triphenylamine group. The other polyimides showed similar CV curves to that of **6e**. The energy levels of the HOMO and LUMO of the investigated polyimides can be estimated from the oxidation onset (E_{onset}) or $E_{1/2}$ value and the onset wavelength (λ_{onset}) of the UV–vis absorption spectra, and the results are also listed in Table 4. The $E_{1/2}$ value of ferrocene/ferrocenium (Fc/Fc^+) is known to be 4.8 eV below the vacuum level and was used as a calibration reference. Thus, the HOMO levels for polyimides **6a**–**6f** were evaluated to be 4.93–5.01 eV and 5.06–5.10 eV calculated from E_{onset} and $E_{1/2}$, respectively. The lower ionization potential could suggest an easier hole-injection into films from ITO electrodes in electronic device applications. Traditionally, introduction of triarylamine units in conjugated polymers was found to effectively enhance the hole-injecting properties of the resulting materials [49,50].

3.2.4. Spectroelectrochemical and electrochromic properties

Spectroelectrochemical experiments were conducted to elucidate the optical characteristics of the electrochromic films. The

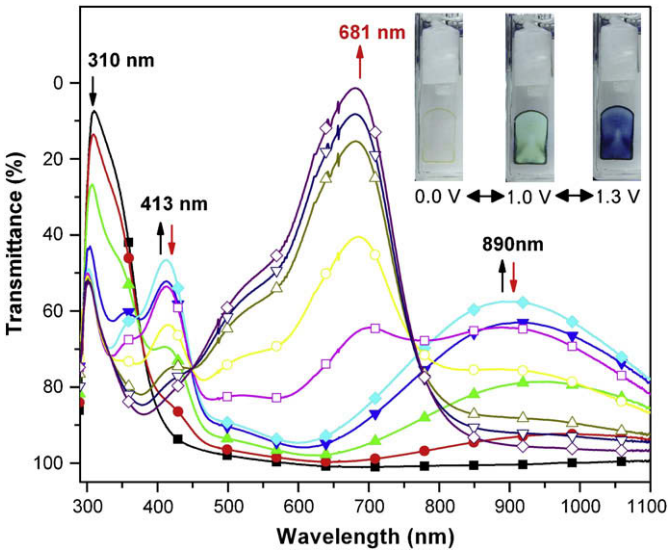

Fig. 7. Spectral change of the cast film of polyimide **6e** on the ITO-coated glass substrate (in acetonitrile with 0.1 M TBAP as the supporting electrolyte) along with increasing applied voltages: 0.0 (■), 0.7 (●), 0.8 (▲), 0.9 (▼), 1.0 (◆), 1.1 (□), 1.15 (○), 1.2 (△), 1.25 (▽) and 1.3 V (◇) (vs. Ag/AgCl couple as reference).

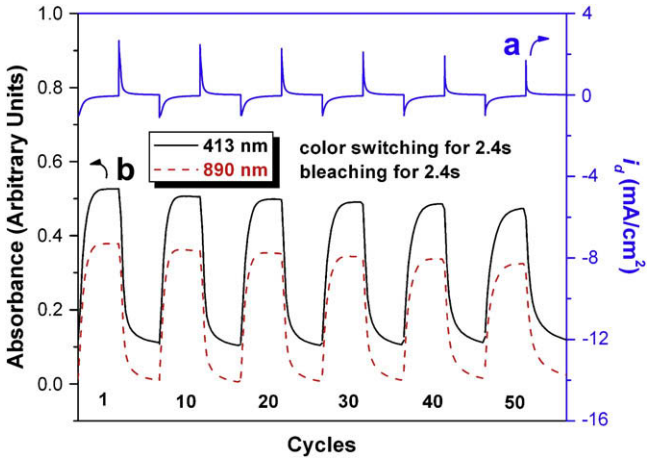

Fig. 8. (a) Current consumption and (b) electrochromic switching between 0 V and 1.0 V and optical absorbance change monitored at 413 and 890 nm for polyimide **6e** in 0.1 M TBAP/CH_3CN with a cycle time of 18 s.

electrode preparations and solution conditions were identical to those used in CV. The typical absorption spectral changes of polyimide **6e** are depicted in Fig. 7. In its neutral state, the film exhibited strong absorption at wavelength around 310 nm, characteristic for triarylamine, but it was almost transmissive in the visible region. When the applied potentials increased positively from 0 to 1.0 V, the absorption peak at 310 nm, characteristic for neutral form polyimide **6e** decreased gradually, and two new bands grew up at 413 and 890 nm due to the first stage oxidation. The new spectrum was assigned as that of the cationic radical of polyimide **6e**. When the potential was adjusted to a more positive value of 1.3 V, corresponding to the second step oxidation, the peak of characteristic absorbance of the radical cation decreased gradually and one new strong absorption band centered at 681 nm grew up. The new spectrum was assigned as a diaction of polyimide **6e**. From the inset shown in Fig. 7, it can be seen that the film of polyimide **6e** switches from a transmissive neutral state (colorless) to a highly absorbing semi-oxidized state (green) and a fully oxidized state (blue). Polyimide **6e** exhibited high optical contrast of percentage transmittance change ($\Delta\%T$) up to 44% at 413 nm and 43% at 890 nm for green coloring and 98% at 681 nm for blue coloring.

The color-switching times were estimated by applying a potential step, and the absorbance profiles were followed (Figs. 8 and 9).

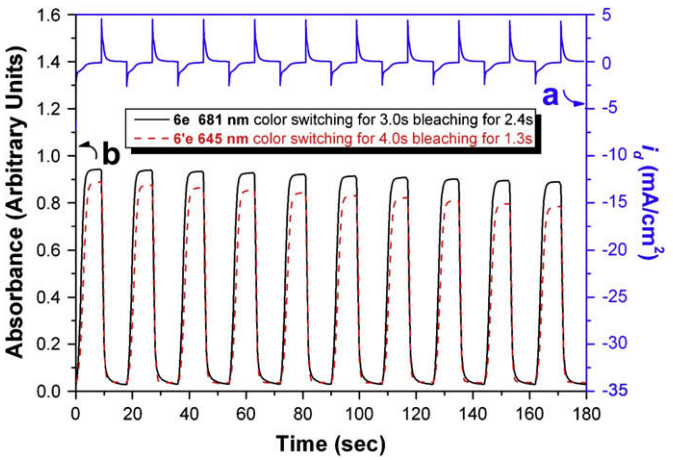

Fig. 9. (a) Current consumption and (b) electrochromic switching between 0 V and 1.0 V and optical absorbance change monitored at 681 and 645 nm for polyimides **6e** and **6′e** in 0.1 M TBAP/CH_3CN with a cycle time of 18 s.

Table 5
Coloration efficiency with optical and electrochemical data of polyimide **6e**.

Cycles[a]	δOD_{890}[b]	Q (mC/cm^2)[c]	η (cm^2/C)[d]	Decay (%)[e]
1	0.366	1.71	214	0
10	0.351	1.66	211	1.4
20	0.337	1.61	209	2.3
30	0.319	1.54	207	3.3
40	0.301	1.46	206	3.7
50	0.284	1.40	203	5.1

[a] Times of cyclic scan by applying potential steps between 0 V and 1.0 V (vs. Ag/AgCl).
[b] Optical density change at 890 nm.
[c] Ejected charge, determined from the *in situ* experiments.
[d] Coloration efficiency is derived from the equation: $\eta = \delta OD_{890}/Q$.
[e] Decay of coloration efficiency after various cyclic scans.

The switching time was calculated at 90% of the full switch because it is difficult to perceive any further color change with naked eye beyond this point. The polyimide switched rapidly (within 3 s) between the highly transmissive neutral state and the colored oxidized state. Thin films from polyimide **6e** would require 2.4 s at 1.0 V for switching absorbance at 413 and 890 nm and 2.4 s for bleaching. When the potential was set at 1.3 V, thin films from polyimide **6e** would require almost 3 s for coloration at 681 nm and 2.4 s for bleaching. After over 50 cyclic scans between 0.0 and 1.0 V, the polymer films still exhibited good electrochemical and electrochromic stability. Coloration efficiency (CE; η) was measured by monitoring the amount of ejected charge (Q) as a function of the change in optical density (ΔOD) of the polymer film [46,47]. The electrochromic coloration efficiencies ($\eta = \Delta OD/Q$) of the polymer films of **6e** after various switching cycles are summarized in Table 5. Polyimide **6e** exhibited high CE values ranging from 214 cm^2/C for the first cycle to 203 cm^2/C for the 50th cycle. After switching 50 times between 0 V and 1.0 V, the film of polyimide **6e** only showed 5.1% decay on CE. After switching 10 times between 0 V and 1.3 V, the film of polyimide **6e** showed a higher electrochromic stability than the corresponding **6′e** counterpart. Therefore, the results of these experiments revealed that the introduction of the *tert*-butyl group at the active sites of the TPPA unit enhances the redox and electrochromic stability of these polymers.

4. Conclusions

A novel class of aromatic polyimides bearing *tert*-butyl-blocked *N*,*N*,*N*′,*N*′-tetraphenyl-1,4-phenylenediamine (TPPA) moieties was prepared by the conventional two-step method from the newly diamine monomer **4** with various tetracarboxylic dianhydrides. The introduction of the bulky *tert*-butyl substituents at the *para*-position of pendent phenyl rings not only stabilized TPPA cationic radicals and dications but also disrupted the coplanarity of aromatic units in chain packing. All the polymers were amorphous with good solubility in many polar organic solvents and exhibited excellent film-forming ability. In addition to high T_g or T_s values and good thermal stability, the polyimides also showed good electrochemical and electrochromic stability. They could change color from the colorless or pale yellowish neutral form to the green and blue oxidized forms. After over fifty cyclic switches, the polymer films still exhibited excellent reversibility of redox and electrochromic characteristics. Thus, these polyimides may find optoelectronic applications as new promising hole-transporting or electrochromic materials.

Acknowledgments

The authors are grateful to the *National Science Council* of the *Republic of China* for the financial support (Grant No. NSC 97-2221-E-027-113-MY3).

References

[1] Monk PMS, Mortimer RJ, Rosseinsky DR. Electrochromism: fundamentals and applications. Weinheim, Germany: VCH; 1995.
[2] Monk PMS, Mortimer RJ, Rosseinsky DR. Electrochromism and electrochromic devices. Cambridge, UK: Cambridge University Press; 2007.
[3] Cronin JP, Gudgel TJ, Kennedy SR, Agrawal A, Uhlmann DR. Mater Res 1999;2:1.
[4] Cummins D, Boschloo G, Ryan M, Corr D, Rao SN, Fitzmaurice D. J Phys Chem B 2000;104:11449.
[5] Heuer HW, Wehrmann R, Kirchmeyer S. Adv Funct Mater 2002;12:89.
[6] Sonmez G, Wudl F. J Mater Chem 2005;15:20.
[7] Rosseinsky DR, Montimer RJ. Adv Mater 2001;13:783.
[8] Mortimer RJ. Chem Soc Rev 1997;26:147.
[9] Sonmez G, Meng H, Wudl F. Chem Mater 2004;16:574.
[10] Sonmez G, Sonmez HB, Shen CKF, Jost RW, Rubin Y, Wudl F. Macromolecules 2005;38:669.
[11] Wu CG, Lu MI, Chang SJ, Wei CS. Adv Funct Mater 2007;17:1063.
[12] Durmus A, Gunbas GE, Toppare L. Chem Mater 2007;19:6247.
[13] Thompson BC, Schottland P, Zong K, Reynolds JR. Chem Mater 2000;12:1563.
[14] Groenendaal L, Zotti G, Aubert PH, Waybright SM, Reynolds JR. Adv Mater 2003;15:855.
[15] Walczak RM, Reynolds JR. Adv Mater 2006;18:1121.
[16] Wilson D, Stenzenberger HD, Hergenrother PM, editors. Polyimides. London: Blackie; 1990.
[17] Sroog CE. Prog Polym Sci 1991;16:561.
[18] Ghosh MK, Mittal KL, editors. Polyimides: fundamentals and applications. New York: Marcel Dekker; 1996.
[19] Huang SJ, Hoyt AE. Trends Polym Sci 1995;3:262.
[20] de Abajo J, de la Campa JG. Adv Polym Sci 1999;140:23.
[21] Eastmond GC, Gibas M, Paprotny J. Eur Polym J 1999;35:2097.
[22] Ayala D, Lozano AE, de Abajo J, de la Campa JG. J Polym Sci Part A Polym Chem 1999;37:805.
[23] Reddy DS, Chou CH, Shu CF, Lee GH. Polymer 2003;44:557.
[24] Yin DX, Li YF, Yang HX, Yang SY, Fan L, Liu JG. Polymer 2005;46:3119.
[25] Lin CH, Lin CH. J Polym Sci Part A Polym Chem 2007;45:2897.
[26] Zhang QY, Chen G, Zhang SB. Polymer 2007;48:2250.
[27] Zhu YQ, Zhao PQ, Cai XD, Meng WD, Qing FL. Polymer 2007;48:3116.
[28] Zhang Q, Li SH, Li WM, Zhang SB. Polymer 2007;48:6246.
[29] Chern YT, Tsai JY. Macromolecules 2008;41:9556.
[30] Liou GS, Hsiao SH, Ishida M, Kakimoto M, Imai Y. J Polym Sci Part A Polym Chem 2002;40:3815.
[31] Liaw DJ, Hsu PN, Chen WH, Lin SL. Macromolecules 2002;35:4669.
[32] Hsiao SH, Chang YM, Chen HW, Liou GS. J Polym Sci Part A Polym Chem 2006;44:4579.
[33] Li WM, Li SH, Zhang QY, Zhang SB. Macromolecules 2007;40:8205.
[34] Thelakkat M. Macromol Mater Eng 2002;287:442.
[35] Cheng SH, Hsiao SH, Su TH, Liou GS. Macromolecules 2005;38:307.
[36] Beaupre S, Dumas J, Leclerc M. Chem Mater 2006;18:4011.
[37] Seo ET, Nelson RF, Fritsch JM, Marcoux LS, Leedy DW, Adams RN. J Am Chem Soc 1966;88:3498.
[38] Nelson RF, Adams RN. J Am Chem Soc 1968;90:3925.
[39] Zhao HD, Tanjutco C, Thayumanavan S. Tetrahedron Lett 2001;42:4421.
[40] Ito A, Ino H, Tanaka K, Kanemoto K, Kato T. J Org Chem 2002;67:491.
[41] Chiu KY, Su TH, Huang CW, Liou GS, Cheng SH. J Electroanal Chem 2005;578:283.
[42] Chang CW, Liou GS. J Mater Chem 2008;8:5638.
[43] Liou GS, Chang CW. Macromolecules 2008;41:1667.
[44] Chang CW, Chung CH, Liou GS. Macromolecules 2008;41:8441.
[45] Hsiao SH, Liou GS, Wang HM. J Polym Sci Part A Polym Chem, in press, doi:10.1002/pola.23323.
[46] Gaupp CL, Welsh DM, Rauh RD, Reynolds JR. Chem Mater 2002;14:3964.
[47] Mortimer RJ, Reynolds JR. J Mater Chem 2005;15:2226.
[48] Demas JN, Crosby GA. J Phys Chem 1971;75:991.
[49] Liang FS, Pu YJ, Kurata T, Kido J, Nishide H. Polymer 2005;46:3767.
[50] Zhao QH, Kim YH, Dang TTM, Shin DC, You H, Kwon SK. J Polym Sci Part A Polym Chem 2007;45:341.